Special Collection

Directed Electron Transfer in Flavin Peptides with Oligoproline-Type Helical Conformation as Models for Flavin-Functional Proteins

Samantha Wörner,[a] Julia Leier,[b] Nadine C. Michenfelder,[b] Andreas-Neil Unterreiner,[b] and Hans-Achim Wagenknecht*[a]

To mimic the charge separation in functional proteins we studied flavin-modified peptides as models. They were synthesized as oligoprolines that typically form a polyproline type-II helix, because this secondary structure supports the electron transfer properties. We placed the flavin as photoexcitable chromophore and electron acceptor at the N-terminus. Tryptophans were placed as electron donors to direct the electron transfer over 0–3 intervening prolines. Spectroscopic studies revealed competitive photophysical pathways. The reference peptide without tryptophan shows dominant non-specific ET dynamics, leading to an ion pair formation, whereas peptides with tryptophans have weak non-specific ET and intensified directed electron transfer. By different excitation wavelengths, we can conclude that the corresponding ion pair state of flavin within the peptide environment has to be energetically located between the S_1 and S_4 states, whereas the directed electron transfer to tryptophan occurs directly from the S_1 state. These photochemical results have fundamental significance for proteins with flavin as redoxactive cofactor.

1. Introduction

Photoinduced charge separation in proteins and charge transport over long distances initiate important biological functions such as respiration and photosynthesis.[1] A fundamental understanding of such electron transfer (ET) processes in proteins is crucial. Long-distance ETs in proteins cannot occur in one step, but typically proceed in a series of hops.[2] Such hopping processes reduce the distance for single ET events and increase the rate of the overall process.[2a] Redox-active amino acids play the role of stepping stones for electron hopping in proteins. In particular, tryptophan (Trp) and tyrosine (Tyr) are most easily oxidized and thus a requisite of electron hole hopping in proteins, in particular with regard to protein-coupled charge transport.[3] For instance, the formation of Tyr radicals is an important part of the ET mechanism in photosystem II, ribonucleotide reductase and cytochrome c oxidase.[4]

Peptides play an important role as electron transport models for fundamental studies.[5] In particular helical scaffolds are promising secondary structure elements for catalysis and ET.[6] Peptides are easily synthesized and modified. We chose a flavin-modified amino acid, which will be named flavin in the following for better readability, as photoinducable electron acceptor in our model peptides since flavin acts as photoinducable and redox active cofactor[7] in important proteins such as cryptochrome blue-light receptors; they are responsible for biochemical photoinduced processes, including morphogenesis and circadian rhythm,[8] and photolyases that repair UV-induced DNA damages.[9] Flavins can be selectively photoexcited in the visible light range and have very distinct and powerful redox properties in three different charge transfer states.[7b,10] Moreover, flavins are able to undergo ET with trytophans and tyrosines as electron donors, which plays a major role in the generation of the fully reduced state of flavins in DNA photolyases[11] and the functional mechanism of cryptochromes.[11c,12] Herein, we present flavin-modified peptides **P1**–**P3** and **P0a**–**P0b** (Figure 1) as models to study and mimic the charge separation and directed ET in functional proteins from Trp and Tyr to the photoexcited flavin. Their functional characterization was elucidated by means of optical spectroscopy.

These peptides are based on the oligoproline scaffold that typically forms a polyproline type-II helix. This secondary structure is important for ET studies in peptides[13] because theoretical studies support the charge-conducting properties[14] and identify prolines as charge stabilizing amino acid.[15] We placed the flavin as electron acceptor (=electron hole donor) at the N-terminus to promote the ET by the intrinsic peptide

[a] Dr. S. Wörner, Prof. H.-A. Wagenknecht
Institute of Organic Chemistry
Karlsruhe Institute of Technology (KIT)
Fritz-Haber-Weg 6
76131 Karlsruhe (Germany)
E-mail: Wagenknecht@kit.edu
[b] J. Leier, N. C. Michenfelder, Dr. A.-N. Unterreiner
Institute of Physical Chemistry
Karlsruhe Institute of Technology (KIT)
Fritz-Haber-Weg 2
76131 Karlsruhe (Germany)

Supporting information for this article is available on the WWW under https://doi.org/10.1002/open.202000199

This article is an invited contribution to a Special Collection highlighting the latest research of ChemistryOpen's Board Members"

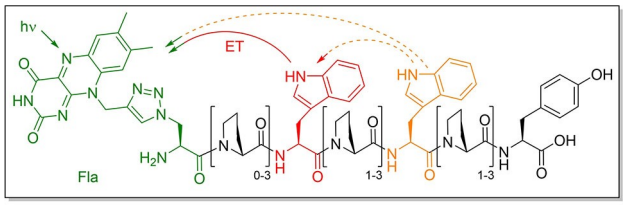

P1: Fla-Pro-Trp-Pro-Trp-Pro-Tyr
P2: Fla-$(Pro)_2$-Trp-$(Pro)_2$-Trp-$(Pro)_2$-Tyr
P3: Fla-$(Pro)_3$-Trp-$(Pro)_3$-Trp-$(Pro)_3$-Tyr
P0a: Fla-Trp-Pro-Trp-Pro-Tyr
P0b: Fla-Trp-$(Pro)_2$-Trp-$(Pro)_2$-Tyr
P0c: Fla-Trp-$(Pro)_3$-Trp-$(Pro)_3$-Tyr

PR: Fla-$(Pro)_3$-Ala-Ala-$(Pro)_3$-Ala

Figure 1. General structure and sequences of model peptides **P1**–**P3** and **P0a**–**P0c** based on oligoprolines with flavin-modified amino acid (Fla, green) at the N-terminus as electron acceptor and tryptophan (Trp, red and orange) as electron donor. In between the donor and acceptor one to three prolines (Pro, black) are located. At the C-terminus the amino acid tyrosine (Tyr, black) is sited. In the reference peptide **PR** the Trps are replaced by alanines (Ala).

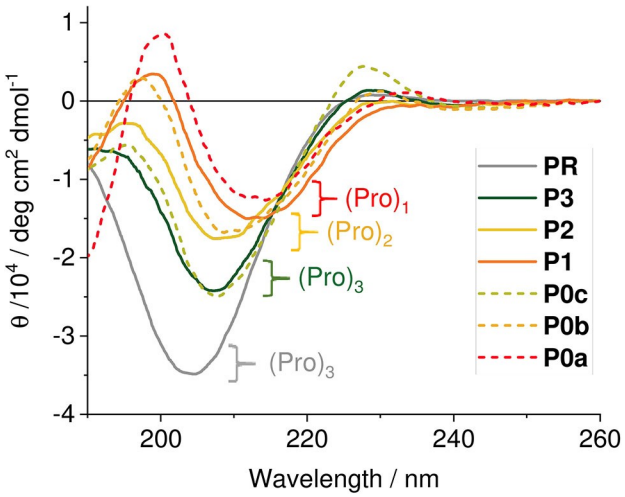

Figure 2. Circular dichroism (CD) of peptides **PR**, **P1**–**P3** and **P0a**–**P0c** (0.1 mg/mL) in MeCN:H_2O = 1:1 at 20 °C.

dipole.[16] Trps were placed with 1–3 intervening prolines in **P1**–**P3** and serve as electron donors (=electron hole acceptors) to direct the electron transfer. In **P0a**–**P0c** the Trp is placed directly adjacent to the flavin amino acid. Peptide **PR** serves as reference peptide without Trp as electron donor.

2. Results and Discussion

To modify peptides by flavin we followed a more convergent approach using the Cu(I)-catalyzed "click"-type azide-alkyne cycloaddition, in contrast to the previously published flavin amino acid derived from L-lysine.[17] The fluorenylmethoxycarbonyl (Fmoc)-protected flavin amino acid building block (Fla) was obtained similarly to our previous approach of attaching pyrenes[18] and aminophthalimide[19] by Cu(I)-catalyzed cycloaddition of the commercially available Fmoc-protected β-azido-L-alanine and the propargyl-substituted flavin (Schemes S1–S4 and Figures S1–14).[20] Fmoc is a protecting group for the amino group of amino acid building blocks. The resulting flavin-modified amino acid building block was incorporated into the peptides **PR**, **P1**–**P3** and **P0a**–**P0c** using standard Fmoc-based solid-phase peptide synthesis protocols. The peptides were purified by reversed-phase HPLC and identified by MS (ESI-TOF). The UV/Vis absorption spectra (Figure S15) show the flavin chromophores in the oxidized state by their characteristic bands with maxima at 362 nm and 442 nm.

The secondary structure of the flavin-modified peptides was studied by CD spectroscopy. The spectra of the reference peptide **PR** show the characteristic line shape for the polyproline type-II helix (Figure S32) with a strong negative signal at 205 nm and a weak positive signal at 230 nm (Figure 2).[21] In the Trp- and Tyr-containing peptides, the portion of the polyproline helix is reduced in comparison to **P3**, but the overall secondary structure clearly depends on the number of proline residues. The intensity of the CD tracks well with the number of prolines in a row that are part of the peptides. The strongest signal is obtained with the reference peptide **PR**, followed by **P3** and **P0c** bearing three prolines adjacent to each other, and **P2** and **P0b** bearing two prolines. The weakest signal is obtained with **P1** and **P0a** due to the presence of only single prolines. The polyproline type-II helix is an extremely stable secondary structure, which is evident from the temperature-dependent CD spectra that show only a slight reduction of the negative band at 205 nm while heating the peptide **PR** to 80 °C (Figure S16).

The fluorescence quantum yield of the reference peptide **PR** ($\Phi_F = 0.290$) is approximately 15-fold higher than that of the flavin-amino acid Fla. This shows that the flavin is embedded in the peptide environment. The fluorescence quantum yield decreases by the Trp in peptides **P1**–**P3** depending on the number of Pro residues as spacer between Fla and Trp, from $\Phi_F = 0.120$ (**P3**) down to $\Phi_F = 0.050$ (**P1**), which indicates fluorescence quenching by electron transfer. In peptides **P0a**–**P0c** the Trp is placed directly adjacent to the flavin chromophore and they show the highest amount of quenching by $\Phi_F = 0.0150$–0.020. Interestingly, there is an additional small influence by the second Trp residue which is placed one Pro (**P0a**), two Pro (**P0b**) and three Pro (**P0c**) away from the first Trp residue.

Accordingly, **P0a** and **P0b** show the lowest amount of fluorescence. The fluorescence lifetimes support the proposal of an electron transfer between Fla and Trp. The lifetime decays must be fitted by means of a biexponential function (results in Table 1). Interestingly, the reference peptide shows a small portion (7%) of the short lifetime τ_1 indicating an electron transfer within this peptide without the contribution of Trp side chains (*vide infra*). With the number of Pro residues between Fla and the first Trp the portion of the short lifetime τ_1 decreases from 54% (**P1**) to 26% (**P3**). Concomitantly, the longer lifetime τ_2 decreases from 4.04 (**P1**) to 3.07 ns (**P0a**). We assign this change of the lifetime τ_2 to the electron transfer between Fla and Trp. Using τ_2 of the reference peptide **PR** as τ_0 we calculated the electron transfer rates according to

$k_{ET} = 1/\tau_2 - 1/\tau_0$. k_{ET} strongly depends on the number of prolines that determine the distance between Fla and the first Trp in the helix. Again, there is a clearly detectable influence of the second Trp in **P0a** since the electron transfer rates in **P0b** and **P0c** are lower and these peptides differ only by the additional prolines between the first and second Trp.

Fluorescence and electron transfer (ET) are competitive dynamics as the relative amplitudes (Table 1) show. Further superimposed relaxation pathways like internal conversion (IC) or intersystem crossing (ISC) to triplet states may occur. To elucidate the photophysical pathways, we recorded transient absorption spectra after 345 and 400 nm excitation for the flavin-modified peptides **PR**, **P1**–**P3** and **P0a**–**P0c** in MeCN:H_2O = 1:1. The basic experimental description is placed in the Supporting Information (Figure S17), while the details have been described previously.[22] The stationary spectra for the presented flavin-modified peptides are similar and show peaks at 362 and 442 nm for absorption as well as 522 nm for emission (Figure S15). In analogy to similar literature known flavins,[10,23] the absorption peaks can be assigned to S_0 –S_2 and S_0 –S_1 transitions and the emission, following Kasha's rule,[24a–b] to $S_1 \rightarrow S_0$, respectively. Therefore, an excitation with 345 nm leads to population of higher singlet states S_2–S_4,[24c] whereby 400 nm excites S_1 and some S_2.[24c]

To understand the complex excited state dynamics of flavin in the peptide environment, we first analyzed the reference system **PR**. The TA spectra of **PR** after 345 nm excitation into S_3 (Figure 3) consist of several contributions in the probing range from 350 to 720 nm: The negative band at 420 nm clearly represents ground-state bleaching (GSB) of S_1 (i), but is superimposed by a strong excited state absorption (ESA) around 500 nm (ii). (iii) A corresponding bleaching is not apparent due to another dominant ESA at 375 nm (iv). A negative contribution at 550 nm occurs due to stimulated emission (SE) (v), which is also superimposed by ESA being obvious beyond 650 nm (vi). Due to a lack of an isosbestic point, both ESA around 500 nm and SE at 550 nm originate from the same singlet state, S_1. After 100 ps, the GSB region (ca. 470 nm) shows a rising bleach component (Figure 3 bottom and S18). More precisely, the corresponding single transient decays at 470 nm within a few ps, but decreases again on a 100 ps time scale (Figure 4). This decrease correlates with a reduction of the SE at 550 nm (Figure S18). Due to its spectral position, it can be assigned to emissions from the hydroquinone forms Fl^- and/or FlH_2 of the flavin with maxima at 450 and 470 nm, respectively,[23a,25] named SE_2. Those should be formed within a few ps. Recent studies suggested[10] that both species can be formed via triplet state dynamics from the excited flavin or via a non-specific ET and are therefore competitive relaxation pathways to ET from Trp to the excited flavin occurring in the singlet state.[10] This decrease at 470 nm is strongest for the reference **PR**, followed by **P3**. The other peptides **P1**–**P2** and **P0a**–**P0c** show minor responses as can be seen in Figure 4 for three proteins (**P1** and **P0a** in Figure S19).

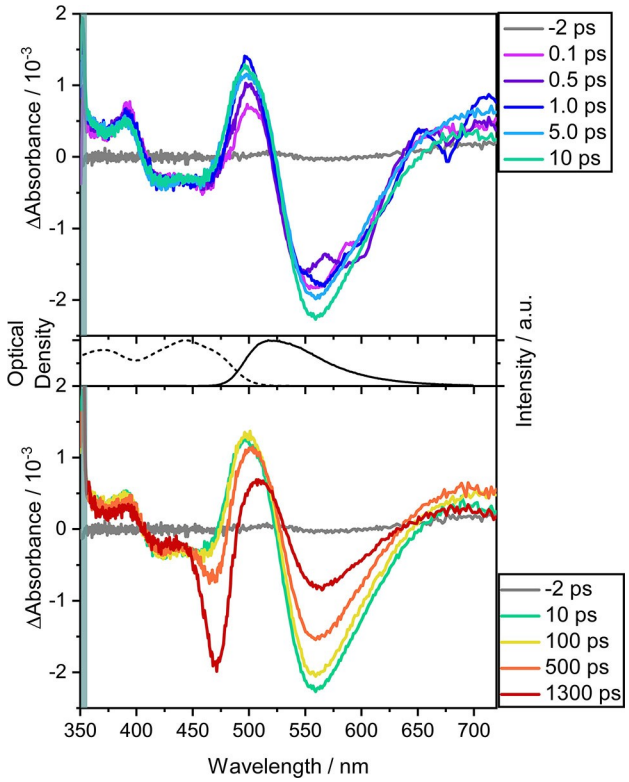

Figure 3. Transient absorption spectra after 345 nm (0.18 μJ, OD = 1.4) excitation of **PR** in MeCN:H_2O = 1:1 at selected relative delay times as indicated and probed between 350 and 720 nm. The grey bar at 350 nm masks the scattering of the pump pulse. Top: Highlighting of early-time dynamics up to 10 ps and, in addition, the corresponding normalized absorption (dotted line) and emission (solid line) spectra in the middle. Bottom: Transients from delay times of −2 ps to 1300 ps.

Table 1. Fluorescence quantum yields Φ_F, fluorescence lifetimes τ_1 und τ_2 (with amplitudes) and the rate constants k_{ET} for the electron transfer in the flavin-modified peptides (P) **PR**, **P1**–**P3** and **P0a**–**P0c** (0.01 mM) in MeCN:H_2O = 1:1

P	Φ_F[a,b]	τ_1 [ns]	rel. Amp. [%]	k_1 [ns^{-1}]	τ_2 [ns]	rel. Amp. [%]	k_{ET} [ns^{-1}]
PR	0.290	1.05	7		5.65[d]	93	
P3	0.120	1.24	26	–[c]	4.04	74	0.070
P2	0.050	1.20	45	–[c]	3.26	55	0.130
P1	0.038	1.10	54	–[c]	3.41	46	0.116
P0c	0.020	1.03	52	0.019	3.07	48	0.148
P0b	0.015	0.99	66	0.058	3.07	34	0.148
P0a	0.016	0.86	46	0.210	2.62	54	0.205

[a] λ_{exc} = 440 nm, λ_{em} = 520 nm. [b] Steady-state fluorescence spectra in Figure S15. [c] Negative values not usable. [d] = τ_0.

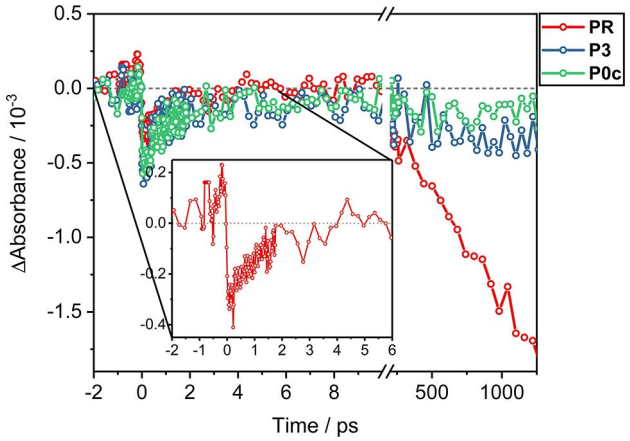

Figure 4. Comparison of single transients at 470 nm of **PR**, **P3** and **P0c** in MeCN:H_2O = 1:1. Excitation at 345 nm with 0.18 μJ at an OD = 1.4, 0.6 and 0.7, respectively. The inset highlights the rising GSB for **PR**. Lines between specific delay times are to guide the eye. The grey dashed line indicates the transient absorption zero.

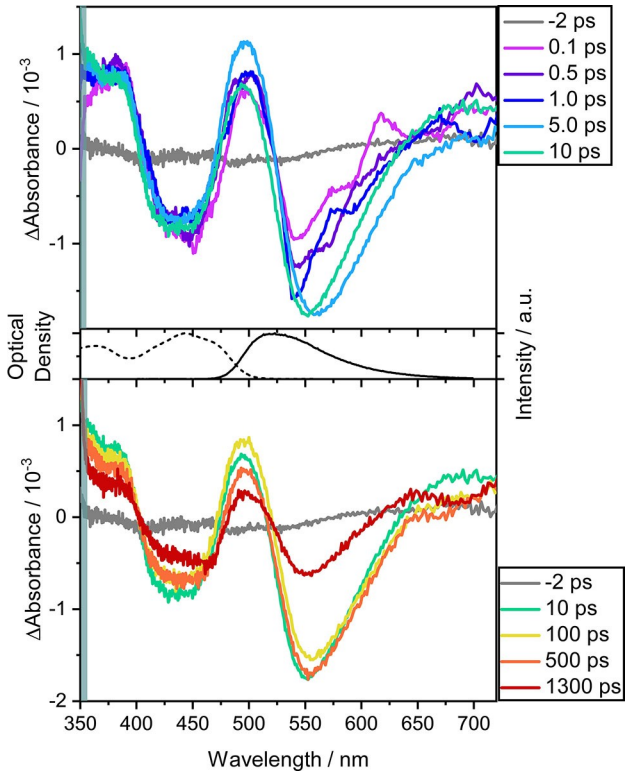

Figure 5. Transient absorption spectra after 345 nm (0.18 μJ, OD = 0.6) excitation of **P3** in MeCN:H_2O = 1:1 at selected relative delay times as indicated and probed between 350 and 720 nm. The grey bar at 350 nm masks the scattering of the pump pulse. Top: Highlighting of early-time dynamics up to 10 ps and, in addition, the corresponding normalized absorption (dotted line) and emission (solid line) spectra in the middle. Bottom: Transients from delay times of −2 ps to 1300 ps.

Selected single transients describe the major transient contributions in **PR** (Figure S18). The dominating ESA band at 500 nm, being superimposed by GSB and SE, does not show an instantaneous but delayed rise within 2 ps indicating excited state molecular motions. Both ESA bands at 370 and 500 nm as well as the GSB around 420 nm decrease to 44% after 1.2 ns from their corresponding maximum or minimum values. This is different for the SE dynamic (at 555 nm), which decays considerably faster. After 1.2 ns, 80% of the initial population recovered, suggesting a competitive channel, e.g. the excited singlet state ET.[10] In contrast to these contributions, the ESA band around 675 nm does not decay significantly within 1.2 ns and points to longer-lived states such as triplet state population. Except for ESA beyond 650 nm, all dynamics show two decay time constants, a short one, $\tau_1 \approx 1$ *ps*, and a longer time constant, $\tau_2 \approx 1$ *ns*. While the first one can be assigned to excited state relaxation processes, the latter is in good agreement with the shorter lifetime of the excited state measured via TCSPC (cf. τ_1 in Table 1). For probe wavelengths above 650 nm, the decay ($\tau_3 \gg 2$ *ns*) exceeds the maximum delay of our experimental setup and supports the idea of a long-living absorption within this wavelength regime. These findings imply that **PR** indeed is a reference system with less directed ET, but favored formation of the hydroquinone form of flavin after higher state excitation, which emits at 470 nm after 100 ps. Its formation can in principle be realized by an ISC[10] or non-specific ET.[25] While flavins usually show ISC on a ns time scale,[10,26a] the deprotonated forms converts on the order of 100 ps,[26b] still being longer than the observed time range of 1 ps. In contrast, non-specific ET is driven via an edge-to-edge tunneling for short distances within 25 ps or shorter, depending on the ion contact pair distance.[26c] Therefore, ultrafast non-specific ET can be a competing pathway to direct ET with Trp.

To apply and compare these findings, **P1**–**P3** and **P0a**–**P0c** were analyzed and show similar transient spectra after excitation with 345 nm (**P3** in Figure 5, **P1**, **P0a** and **P0c** in Figure S20–S22). **P3** and **P0a** show similar major long-lived contributions as the reference **PR**, like GSB (~420 nm) and SE (~550 nm), as well as ESA around 375, 500 and 675 nm. The main difference is the weaker SE_2 around 470 nm, which has been already discussed above. Obviously, there is less formation of the hydroquinone forms of flavin, which implies less favored non-specific ET than in the reference system **PR**. Furthermore, this dynamic is more dominant in **P3** than in **P0a**, where only a weak decrease was identified.

In addition to transient spectra with 345 nm excitation, experiments with excitation at 400 nm were carried out under similar conditions, leading to a distributed S_1 and S_2 transition. In general, these spectra exhibit similar dynamics as shown before after an excitation at 345 nm (**PR**, **P1**–**P3** and **P0a**–**P0c** in Figure S23–S29). For the reference **PR**, the negative bands at 420 and 550 nm can be assigned to GSB and SE. Again, no bleaching of S_2 can be detected due to superposition of a dominant ESA at 345 nm, signalizing a long-lived state. Further contributions around 500 and 675 nm are a result of ESA, which superimpose the SE band, resulting in a shifted maxima of SE compared to the emission band. The dominating ESA band at 500 nm rises within few tens ps and decreases on a few hundred ps timescale (Figure S30). Again, the long-lived ESA at 435 nm indicates a triplet state absorption. As for the 345 nm

excitation, the dynamics are longer-living and do not decay within the observed time window of 1.5 ns, with one excemption of the GSB at 470 nm. Though qualitatively similar to the higher excitation energy, there is a considerable difference concerning the extent of the decrease of △A after 100 ps (Figure S30).

In analogy to the discussion above, we assign this much lower emission to the hydroquinone forms of flavin[10] denoted as stimulated emission SE_2. In contrast to the 345 nm experiment, this decrease is not as pronounced and does not correlate with the increase of the SE at 550 nm. Further, the SE relaxes faster due to less excess energy within the excitation. This indicates that within the 400 nm measurement triplet dynamics are not the prevalent relaxation pathways. Since direct ET and non-specific ET are competitive pathways, the direct ET must be strengthened. This leads to the assumption that the excitation with 400 nm is slightly above the barrier of the channel entrance for ET. Hence, the ET state is supposed to be lower than the singlet ion pair state, whereas both states are energetically located in between the S_1 and S_4. A comparison of all flavin peptides reveals that the rise of the negative band at 470 nm is again most dominant in **PR**, followed by **P3. P1–P2** and **P0a–P0c** do only slightly decrease at 470 nm.

Overall, no influence of the Φ_F and the intensity of SE for both excitation wavelengths were identified. Furthermore, the substitution length at the peptide chain does not influence the lifetime or Φ_F, pointing to a steric unhindered peptide chain, which does not quench the excited state lifetime of the compounds. Nevertheless, a negative correlation of the numbers of prolines and the lifetime within the fs measurements has been observed. A closer proximity of flavin and Trp leads to a shorter lifetime, detectable due to the decay of population (Table 2). Therefore specific wavelengths from each contribution (370, 435, 500 and 555 nm) have been analyzed. To demonstrate this effect, single transients at 555 nm for the 345 nm measurement are displayed in Figure S31. For the 345 nm excitation into higher excited stated, we found that only 44% of the excited population of the reference system **PR** relaxed to the ground state after 1.2 ns. For **P3** with three prolines between flavin and Trp, 55% of the population decayed to the ground state, whereas this number increased to 80% with only one proline in **P1**. Though minor, the second Trp and the number of prolines between both Trps influence the lifetime as follows: with a decrease by two prolines, 91% (**P0a**) instead of 85% (**P0c**) of the population relaxes to the ground state. Slightly different values with the same trend were observed in the 400 nm measurements. Here, 43% of the population of **P3** and 80% of **P1** relaxes back. Due to further possible relaxation pathways the values are not absolute, although this trend correlates with the increase of the relative amplitudes A_1 from TCSPC (Table 1), that increases from 7% (**PR**) to 26% (**P3**) with the number of prolines between flavin and Trp.

3. Conclusions

The flavin-modified peptides **P1**–**P3** and **P0a**--**P0b** serve as models to study and mimic the charge separation and ET in functional proteins. These peptides are based on the oligoproline scaffold. The polyproline type-II helix is an advantageous secondary structure for ET in peptides. The flavin as electron acceptor was placed at the N-terminus and two Trps with 0–3 intervening prolines to direct the ET. Spectroscopic studies, especially time-resolved investigations, demonstrated how the number of prolines and thereby the distance between flavin and Trp moieties affect excited state lifetimes as well as the quantum yields. The ET from Trp to the flavin moiety and the formation of the hydroquinone forms $FlavinH^-$ and $FlavinH^-_2$ by non-specific ET are competitive pathways. Since the latter formation involves a ion pair state,[26c] the reference system **PR** shows a dominant non-specific ET whereas **P0a** has a weak non-specific ET (cf. a weak band at 470 nm) and therefore a strengthened *and* directed ET. On the basis of different excitation wavelengths, we can conclude that the corresponding singlet ion pair state has to be energetically located between the S_1 and higher excites states up to S_4, whereas the directed ET to Trp can occur directly from the S_1 (Figure 6). Furthermore, an excitation with 400 nm favors the directed ET from Trp to the flavin moiety. Both, steady-state and time-resolved studies indicate a contribution to directed ET not only by the first Trp but also by the second one, indicating a charge hopping in the peptides. These results underscore the model character of these peptides and their fundamental significance for proteins with flavin as redox active cofactor.

Experimental Section

All experimental details and procedures are described in the Supporting Information.

Table 2. Decay of the population of the flavin oligoprolines after 1.2 ns for excitation wavelength 345 and 400 nm. The values have been gained by selecting wavelengths from each contribution. Therefore, the ratio of the signal intensity to the minima/maxima has been analyzed. The distance between flavin and Trp decreases from top to bottom, except **PR**.

Compound	345 nm	400 nm
PR	(44 ± 1)%	(25 ± 5)%
P3	(55 ± 3)%	(43 ± 1)%
P2	–	(74 ± 3)%
P1	(80 ± 5)%	(80 ± 8)%
P0c	(85 ± 6)%	(82 ± 4)%
P0b	–	(87 ± 6)%
P0a	(91 ± 3)%	(89 ± 7)%

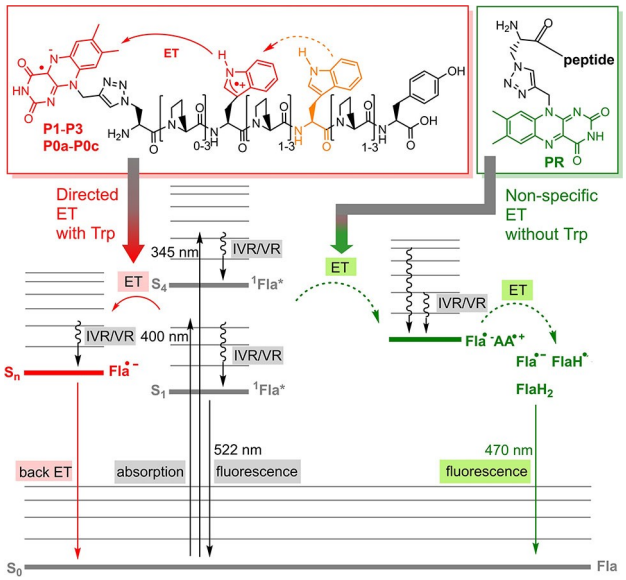

Figure 6. Conclusive Jablonski diagram for the flavin-modified peptides, based also on work from literature.[10,27] Competitive pathways are the non-specific electron transfer (ET) leading to an ion radical pair in the singlet state of the flavin and amino acids (AA) in the reference peptide **PR** (green) and the directed ET in the peptides with Trp **P1**–**P3** and **P0a**–**P0c** (red). Additionally, absorption, fluorescence, phosphorescence, back ET, internal vibrational redistribution (IVR) and vibrational relaxation (VR) are shown (gray). The energies of the singlet and ion radical pair in the singlet states are similar, but subject to small variations resulting in the observation of varying ultrafast dynamics – and thus ET efficiency – of the different oligoproline peptides.

Acknowledgements

Financial support by the Deutsche Forschungsgemeinschaft (GRK 2039/2) and KIT is gratefully acknowledged. Open access funding enabled and organized by Projekt DEAL.

Conflict of Interest

The authors declare no conflict of interest.

Keywords: chromophores · transient absorption spectroscopy · peptides · proteins · electron transfer

[1] H. B. Rgay, J. R. Winkler, *Quart. Rev. Biophys.* **2003**, *36*, 341–372.
[2] a) J. Yu, J. R. Horsley, A. D. Abell, *Acc. Chem. Res.* **2018**, *51*, 2237–2246; b) R. A. Malak, Z. Gao, J. F. Wishart, S. S. Isied, *J. Am. Chem. Soc.* **2004**, *126*, 13888–13889; c) D. N. Beratan, *Annu. Rev. Phys. Chem.* **2019**, *70*, 71–97.
[3] J. L. Dempsey, J. R. Winkler, H. B. Gray, *Chem. Rev.* **2010**, *110*, 7024–7039.
[4] B. A. Barry, *J. Photochem. Photobiol. B* **2011**, *104*, 60–71.
[5] a) M. Cordes, B. Giese, *Chem. Soc. Rev.* **2009**, *38*, 892–901; b) J. Gao, P. Müller, M. Wang, S. Eckhardt, M. Lauz, K. M. Fromm, B. Giese, *Angew. Chem. Int. Ed.* **2011**, *50*, 1926–1930; *Angew. Chem.* **2011**, *123*, 1967–1971; c) A. Shag, B. Adhikari, S. Martic, A. Munir, S. Shahzad, K. Ahmad, H.-B. Kraatz, *Chem. Soc. Rev.* **2015**, *44*, 1015–1027.
[6] T. B. J. Pinter, K. J. Koebke, V. L. Pecoraro, *Angew. Chem. Int. Ed.* **2020**, *59*, 7678–7699.
[7] a) S. L. J. Tan, R. D. Webster, *J. Am. Chem. Soc.* **2012**, *134*, 5954–5964; b) P. F. Heelis, *Chem. Soc. Rev.* **1982**, *11*, 15–39; c) S. Ghisla, W. C. Kenney, W. R. Knappe, W. McIntire, T. P. Singer, *Biochemistry* **1980**, *19*, 2537–2544.
[8] a) C. Lin, D. Shalitin, *Annu. Rev. Plant Biol.* **2004**, *0*; b) R. Stanewsky, *J. Neurobiol.* **2003**, *54*, 111–147.
[9] A. Sancar, *Chem. Rev.* **2003**, *103*, 2203–2237.
[10] U. Megerle, M. Wenninger, R.-J. Kutta, R. Lechner, B. König, E. Riedle, *Phys. Chem. Chem. Phys.* **2011**, *13*, 8869–8880.
[11] a) T. Carell, L. T. Burgdorf, L. M. Kundu, M. Cichon, *Curr. Opin. Chem. Biol.* **2001**, *5*, 491–498; b) M. Müller, T. Carell, *Curr. Opin. Struct. Biol.* **2009**, *19*, 277–285; c) P. Müller, E. Ignatz, S. Kiontke, K. Brettel, L.-O. Essen, *Chem. Sci.* **2018**, *9*, 1200–1212.
[12] a) P. Müller, J. Yamamoto, R. Martin, S. Iwai, K. Brettel, *Chem. Commun.* **2015**, *51*, 15502–15505; b) F. Lacombat, A. Espagne, N. Dozova, P. Plaza, P. Müller, K. Brettel, S. Franz-Badur, L.-O. Essen, *J. Am. Chem. Soc.* **2019**, *2019*, 13394–13409.
[13] D. R. Striplin, S. Y. Reece, D. G. McCafferty, C. G. Wall, D. A. Friesen, B. W. Erickson, T. J. Meyer, *J. Am. Chem. Soc.* **2004**, *126*, 5282–5291.
[14] a) N. P.-A. Monney, T. Bally, B. Giese, *J. Phys. Chem. B* **2015**, *119*, 6584–6590; b) A. Heck, P. B. Woiczikowski, T. Kubar, K. Welke, T. Niehaus, B. Giese, S. Skourtis, M. Elstner, T. R. Steinbrecher, *J. Phys. Chem. B* **2014**, *118*, 4261–4272; c) A. Heck, P. B. Woiczikowski, T. Kubar, B. Giese, M. Elstner, T. B. Steinbrecher, *J. Phys. Chem. B* **2012**, *116*, 2284–2293.
[15] N. P.-A. Monney, T. Bally, B. Giese, *J. Phys. Org. Chem.* **2015**, *28*, 347–353.
[16] E. Galoppini, M. A. Fox, *J. Am. Chem. Soc.* **1996**, *118*, 2299–2300.
[17] T. Carell, H. Schmid, M. Reinhard, *J. Org. Chem.* **1998**, *63*, 8741–8747.
[18] a) S. Hermann, D. Sack, H.-A. Wagenknecht, *Eur. J. Org. Chem.* **2018**, 2204–2207; b) S. Hermann, H.-A. Wagenknecht, *J. Pept. Sci.* **2017**, *23*, 563–566.
[19] S. Wörner, F. Rönicke, A. S. Ulrich, H.-A. Wagenknecht, *ChemBioChem* **2020**, *21*, 618–622.
[20] J. B. Carroll, B. J. Jordan, H. Xu, B. Erdogan, L. Lee, L. Cheng, C. Tiernan, G. Cooke, V. M. Rotello, *Org. Lett.* **2005**, *7*, 2551–2554.
[21] J. L. S. Lopes, A. J. Miles, L. Whitmore, B. A. Wallace, *Protein Sci.* **2014**, *23*, 1765–1772.
[22] a) C. Schweigert, O. Babii, S. Afonin, T. Schober, J. Leier, N. C. Michenfelder, I. V. Komarov, A. S. Ulrich, A. N. Unterreiner, *ChemPhotoChem* **2019**, *3*, 403–410; b) P. Jöckle, C. Schweigert, I. Lamparth, N. Moszner, A.-N. Unterreiner, C. Barner-Kowollik, *Macromolecules* **2017**, *50*, 8894–8906.
[23] a) Y. Ai, C. Zhao, J. Xing, Y. Liu, Z. Wang, J. Jin, S. Xia, G. Cui, X. Wang, *J. Phys. Chem. A* **2018**, *122*, 7954–7961; b) P. C. Andrikopoulos, Y. Liu, A. Picchiotti, N. Lenngren, M. Kloz, A. S. Chaudhari, M. Precek, M. Rebarz, J. Andreasson, J. Hajdu, B. Schneider, G. Fuertes, *Phys. Chem. Chem. Phys.* **2020**, *22*, 6538–6552; c) P. F. Heelis, *Chem. Soc. Rev.* **1982**, *11*, 15–39.
[24] a) M. Kasha, *Discuss. Faraday Soc.* **1950**, 14–19; b) N. J. Turro, V. Ramamurthy, W. Cherry, W. Farneth, *Chem. Rev.* **1978**, *78*, 125–145; c) L. Zanetti-Polzi, M. Aschi, I. Daidone, A. Amadei, *Chem. Phys. Lett.* **2017**, *669*, 119–124.
[25] Y. T. Kao, C. Saxena, T. F. He, L. Guo, L. Wang, A. Sancar, D. Zhong, *J. Am. Chem. Soc.* **2008**, *130*, 13132–13139.
[26] a) S. Salzmann, J. Tatchen, C. M. Marian, *J. Photochem. Photobiol. A* **2008**, *198*, 221–231; b) G. Li, K. D. Glusac, *J. Phys. Chem. A* **2008**, *112*, 4573–4583; c) C. Bialas, D. T. Barnard, D. B. Auman, R. A. McBride, L. E. Jarocha, P. J. Hore, P. L. Dutton, R. J. Stanley, C. C. Moser, *Phys. Chem. Chem. Phys.* **2019**, *21*, 13453–13461.
[27] C.-Y. Lu, Y.-Y. Liu, *BBA - General Subjects* **2002**, *1571*, 71–76.

Manuscript received: July 10, 2020
Revised manuscript received: October 23, 2020